The effects of detwinning on the mechanical properties of AZ31B magnesium alloy with different strain rates at 423 K

Lifei Wang [a,c], Guangsheng Huang [a,*], Zhaoyang Shi [a], Hua Zhang [a], Paola Bassani [b], Maurizio Vedani [c], Fusheng Pan [a]

[a] College of Materials Science and Engineering, Chongqing University, Chongqing 400045, China
[b] Institute for Energetics and Interphases, National Research Council, 23900 Lecco, Italy
[c] Department of Mechanical Engineering, Politecnico di Milano, 20156 Milan, Italy

Received 26 February 2014
Received in revised form
13 May 2014
Accepted 21 June 2014
Available online 28 June 2014

1. Introduction

Due to the high specific strength, high stiffness and low density, magnesium alloys are attractive materials for structural and functional applications in automotive sector, electronic device industry and many other fields of large mass production [1,2]. However, magnesium alloys also feature a poor formability at low temperature owing to their HCP structure. At relatively low temperature, magnesium provides only two basal slip systems which cannot fit the Von Mises Criterion requiring five independent slip systems [3,4]. It was demonstrated that only the twinning mechanism could coordinate the deformation along the prismatic direction, showing that twinning plays an important role in the deformation of magnesium alloys at low temperature [5]. It was also reported that the {10–12} twinning is easily generated when the load is applied on specific planes (i.e.: compression parallel to *c*-axis of HCP cells or tension perpendicular to *c*-axis) [6]. Song et al. [7] indicated that the twins could divide the grain boundaries and refine the grain size so that mechanical properties could be improved. However, Wu et al. [8] also reported that detwinning occurred under reversal loading conditions and it played an important effect on the mechanical property of magnesium alloy. Wang et al. [9] pointed out that detwinning was evident on tension straining an AZ31 alloy after pre-compression and resulted in a remarkable drop of the tensile yield strength, from 265 MPa to 160 MPa.

Up to now, the twinning–detwinning behavior of magnesium alloys has been mainly researched under fatigue testing conditions, with a constant strain rate. However, to the authors' knowledge, twinning–detwinning behavior with different strain rates has not yet been investigated under quasi-static loading conditions at temperatures above RT. It is expected that higher strain rate levels would induce increased stress concentration in the crystal structure that could make the twinning generation more favorable [10]. A similar effect could also play a role on detwinning mechanisms as well. To investigate these issues, this paper is focused on the twinning–detwinning behavior at different strain rates of an AZ31 alloy tested at 423 K and on the resulting effects on the mechanical properties.

2. Experimental procedure

In order to obtain a uniform microstructure with a bigger grain size, as-extruded bars of AZ31 magnesium alloy (Mg–3 wt%Al–1 wt%Zn) with a diameter of 16 mm were annealed at 673 K for 3 h firstly. The value of 673 K was selected as a reference temperature

* Corresponding author. Tel.: +86 23 65112239; fax: +86 23 65102821.
E-mail address: Gshuang@cqu.edu.cn (G. Huang).

for annealing of AZ31 Mg alloys [11]. A microstructure with large amount of {10–12} tension twins was obtained by compression strain to 3% (The value of 3% was selected in order to allow comparisons with previous researches, e.g. [12]) along the extrusion direction (ED). The pre-compression tests have been carried out on specimens having a diameter of 16 mm and a length of 105 mm, with a strain rate of $10^{-3}\,s^{-1}$ at room temperature. In order to avoid bending–buckling during compression, the samples were clamped by a special fixture along ED. The schematic diagram was shown in Fig. 1.

As-received and pre-strained under compression AZ31 alloy samples were machined to produce tensile specimens with a nominal gage length of 36 mm and a diameter of 6 mm. Tensile tests were carried out using a CMT6305-300KN electronic universal testing machine with strain rates of $10^{-1}\,s^{-1}$, $10^{-2}\,s^{-1}$, $10^{-3}\,s^{-1}$, $10^{-4}\,s^{-1}$ (common strain rate range, e.g. [13]) at 423 K. It is well known that at temperatures above 473 K, the non-basal slips become active and dynamic recrystallization may also occur. These two mechanisms are expected to have marked effects on microstructure and properties of AZ31Mg alloy especially on the twinning and detwinning [14]. In order to preserve twins in the microstructure and reduce the influence on the detwinning, a lower temperature should be considered [15]. On the other hand, it is also known that at temperatures lower than 423 K, magnesium alloys are not very sensitive to the strain rate. For these reasons a compromise temperature level, specifically of 423 K, has been chosen for this investigation. The specimens were mounted in the testing frame, heated and held at set temperature for 5 min before starting the test. In order to minimize the potential sources of error, each test was repeated three times. Inverse tensile tests on the PRC specimens were performed up to fracture point. In addition, interrupted tensile tests on the same materials were also carried out up to a strain of 5% within the same strain rate range and temperature.

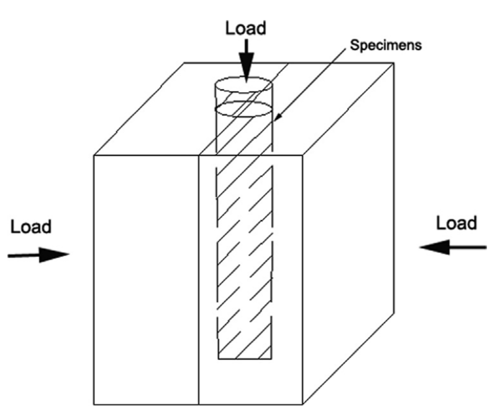

Fig. 1. The schematic diagram of special fixture for pre-compression.

The microstructure and texture of the as-received and PRC samples were characterized by optical microscopy and electron backscatter diffraction (EBSD). The optical microstructure was observed by standard metallographic technique. Samples preparation for EBSD observation consisted in mechanical grinding followed by polishing down to colloidal silica naps. Then electropolishing was performed using a solution of 20% nitric acid and 80% methanol with a voltage of 20 V for 120 s at temperature of −30 °C. Finally, EBSD measurements were performed on a Zeiss EVO 50 SEM. The EBSD data were processed by an INCA OXFORD crystal software.

3. Results and discussion

True stress–strain curves of as-received and pre-deformed 3% samples with different strain rate at 423 K are given in Fig. 2. Mechanical properties derived from the curves are also listed in Table 1. From sets of data on as-received samples, it is confirmed that yield strength (YS), ultimate tensile strength (UTS) decrease and fracture elongation increases with the decrease of strain rate. The biggest elongation is 37.2% at $10^{-4}\,s^{-1}$ which increases by 49.3% than that at $10^{-1}\,s^{-1}$. The same trend was also measured in PRC specimens, YS and UTS decreases as the decrease of strain rate. However, the yield strength just differs slightly. Besides, fracture elongation expresses a different way. The biggest elongation is obtained at $10^{-2}\,s^{-1}$ with a value of 41.9%, then it decreases as the strain rate decreases from 10^{-2} to $10^{-4}\,s^{-1}$.

Comparing as-received and pre-deformed samples, the tension curves of pre-compressed samples present a change of slope that can suggest the onset of a different deformation mechanism. Besides, YS and UTS decrease in the pre-deformed samples at any strain rate. The yield strength decreases even 62 MPa after pre-compression at $10^{-1}\,s^{-1}$. Fracture elongation increases at strain rate of $10^{-2}\,s^{-1}$ and $10^{-3}\,s^{-1}$, except $10^{-1}\,s^{-1}$ and $10^{-4}\,s^{-1}$.

Fig. 3 shows the microstructure and texture of as-received and pre-deformed under compression (PRC) samples. From Fig. 3 (a), it can be demonstrated that in the as-received materials, the microstructure consisted of many equiaxed grains with a size of about 15.5 μm, with no evidence of twins. After deformation to 3% along ED, a large amount of twins appeared in the microstructure, and a texture of twins with c-axial∥ED, as depicted in Fig. 3(b). Fig. 3 (c) shows an enlarged image of 3% PRC sample pre-deformed under compression, it is shown that the lentoid lamellas run

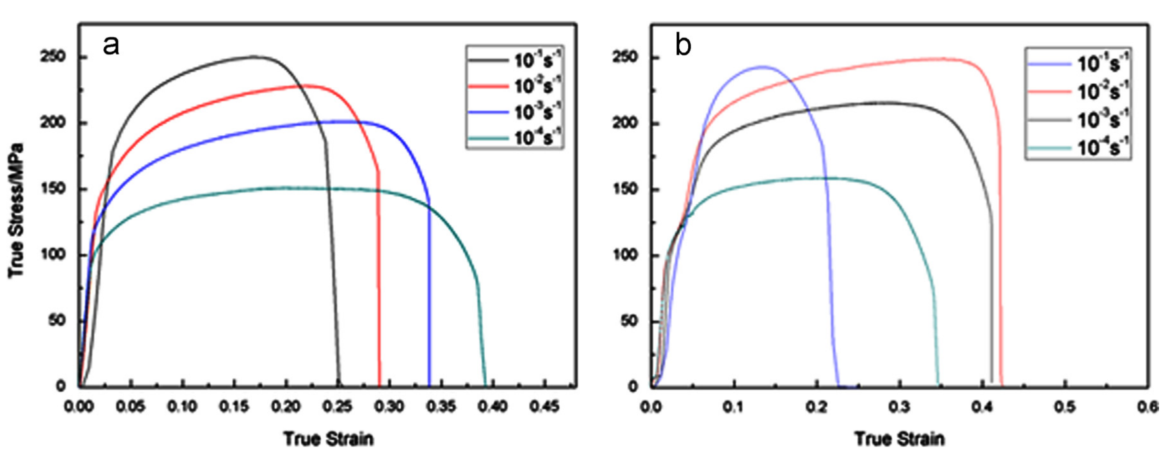

Fig. 2. Stress vs. strain curves of the AZ31 alloy recorded at different strain rates: (a) as-received materials, (b) 3% PRC samples.

through the whole grain. Based on the EBSD data, the boundaries of the lamellas are {10–12} tensile twinning boundaries.

The microstructure of as-received AZ31 magnesium alloy after tensile tests at strain rates of $10^{-1}\,s^{-1}$, $10^{-2}\,s^{-1}$, $10^{-3}\,s^{-1}$, $10^{-4}\,s^{-1}$ is shown in Fig. 4. A higher-magnification view of the microstructure observed in the sample tensile tested at $10^{-4}\,s^{-1}$ is also presented. Comparing with the original microstructure, it can be observed that some small grains are located at the grain boundaries of the coarser crystals. This was accounted by the occurrence of dynamic recrystallization (DRX) at temperature of 423 K [16–18]. As the testing strain rate decreases, the amount of newly recrystallized grains nucleated at grain-boundaries increased. This suggests that the development of new grains by DRX would be favoured by decreasing the strain rate, hence increasing the testing time. Bruni et al. [13] also reported that the DRX has an effect in refining the grain size and a concurrent effect of softening. Due to the softening effect, the flow stress would decrease and the fracture elongation would increase as well at slower strain rates for the enhanced softening effects, as shown in Table 1.

Table 1
Yield strength (YS), Ultimate tensile strength (UTS) and fracture elongation recorded at the indicated stain rates.

	Strain rate (s^{-1})	YS (MPa)	UTS (MPa)	ε_u (%)
As-received	10^{-1}	178 ± 2	250 ± 3	24.9 ± 0.3
	10^{-2}	140 ± 3	228 ± 2	27.1 ± 0.4
	10^{-3}	117 ± 3	201 ± 3	32.4 ± 0.3
	10^{-4}	95 ± 4	146 ± 2	37.2 ± 0.2
PRC	10^{-1}	116 ± 3	245 ± 3	21.3 ± 0.3
	10^{-2}	101 ± 2	236 ± 2	41.9 ± 0.2
	10^{-3}	98 ± 4	213 ± 3	40.8 ± 0.3
	10^{-4}	96 ± 3	151 ± 4	33.0 ± 0.4

Fig. 5 shows the microstructure of PRC specimens after inverse tensile testing as a function of strain rate at 423 K. A large amount of twins is present in the pre-compressed microstructure, however, the twins disappeared after inverse tensile deformation. Song et al. [7] reported that the {10–12} twins would be retained after annealing at a low temperatures, below 473 K. It is therefore supposed that the present disappearance of {10–12} twins would be only related to the detwinning mechanism. Proust et al. [19] pointed out that the detwinning behavior would happen when an inverse load acted on the AZ31 magnesium alloy.

Comparing the set of images of Fig. 5 with Fig. 4, it is revealed that a smaller amount of fine recrystallized grains can be found in the PRC samples than those in as-received materials at each different strain rate. It seems that the DRX was delayed at any strain rate (ranging from $10^{-1}\,s^{-1}$ to $10^{-4}\,s^{-1}$) during inverse tensile testing. Li et al. [20] indicated that the DRX was delayed on rolled and annealed AZ31 rods during the following extrusion, mainly because {10–12} tensile twinning was a dominant deformation mechanism at the initial stage of extrusion. Indeed, it was supposed that, due to the profuse twinning, the stored energy

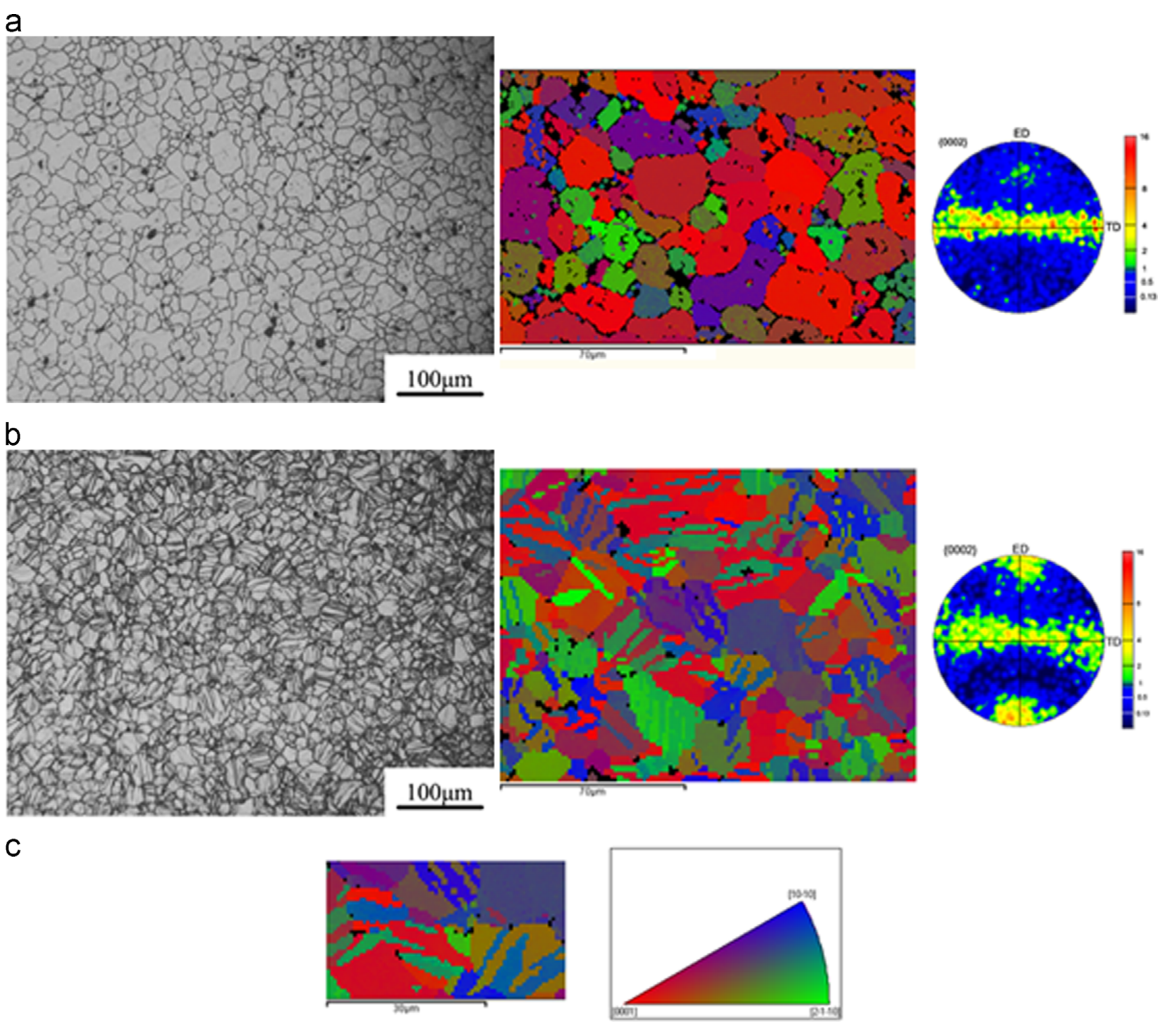

Fig. 3. Representative optical micrographs of AZ31 extruded alloys taken along cross-sectional plane: (a) as-received, (b) 3% PRC, (c) enlarged image of 3% PRC sample.

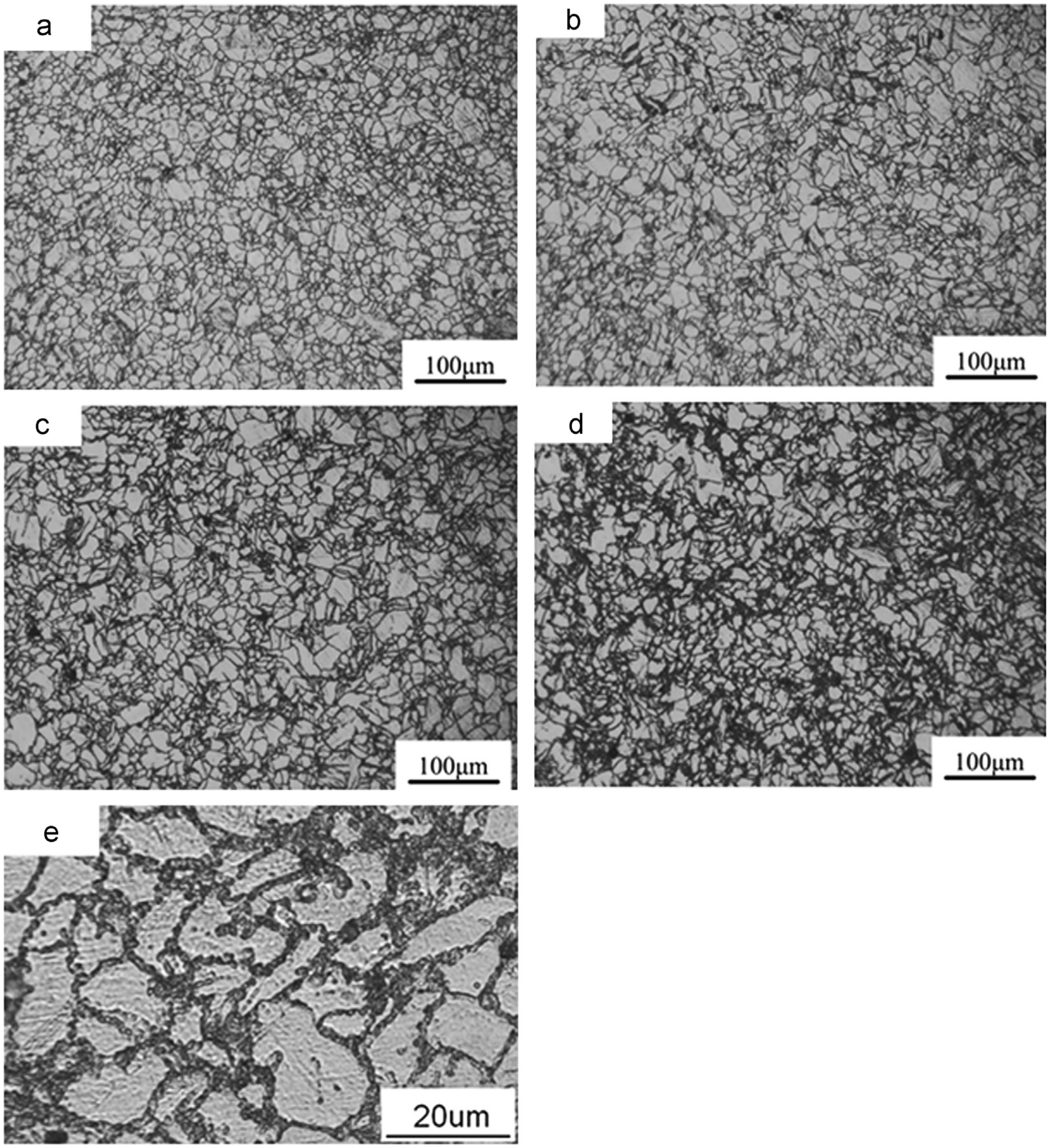

Fig. 4. Optical micrographs of as-received AZ31 magnesium alloy after tensile deformation at different strain rates at 423 K: (a) 10^{-1} s^{-1}, (b) 10^{-2} s^{-1}, (c) 10^{-3} s^{-1}, (d) 10^{-4} s^{-1}, (e) higher magnification image at 10^{-4} s^{-1}.

related to dislocation activity was kept to relatively small amount, so that onset of DRX could be achieved only after much larger strains. It is a very similar phenomenon in the current investigation. Due to the detwinning, and hence recovery of the strain, the stored energy was reduced and larger deformation levels were required to activate DRX, which resulted in the measured delay DRX effect.

In previous state, the yield strength in PRC samples after inverse tensile tests decreases comparing with as-received specimens. This peculiar behavior can be related to the occurrence of the detwinning mechanism. Wang et al. [9] reported that all the strains caused by twinning during compressive deformation on AZ31 extruded magnesium alloy could be recovered in inverse tensile tests, therefore the tensile yielding was mainly dominated by detwinning. Detwinning is similar to the twinning process. However, it may require less energy to be activated because the twins already exist and no nucleation is necessary. In addition, back-stresses accumulated during twin growth, may also aid the detwinning process [21]. So it expresses a smaller YS comparing with as-received material.

As far as the influence of strain rate is concerned, it is recalled that longer times are allowed for restoration (release of work-hardening) at lower strain rates. It is well known, the dynamic recovery would happen at 423 K which causes a softening effect at the same time. A lower strain rate and a longer deformation time, the softening effect would be enhanced as well. So that the yield strength and ultimate tensile strength will be decreased as the strain rate decreases, both in the as-received and PRC samples. However, YS of pre-deformed samples just decreased slightly. It decreased by 15, 3, 2 MPa from 10^{-1} s^{-1} to 10^{-2} s^{-1}, 10^{-3} s^{-1},10^{-4} s^{-1}, respectively. It is far smaller gradient than that in as-received samples. This may because the first dominated deformation mechanism of pre-compressed samples during inverse tensile test is detwinning [12].

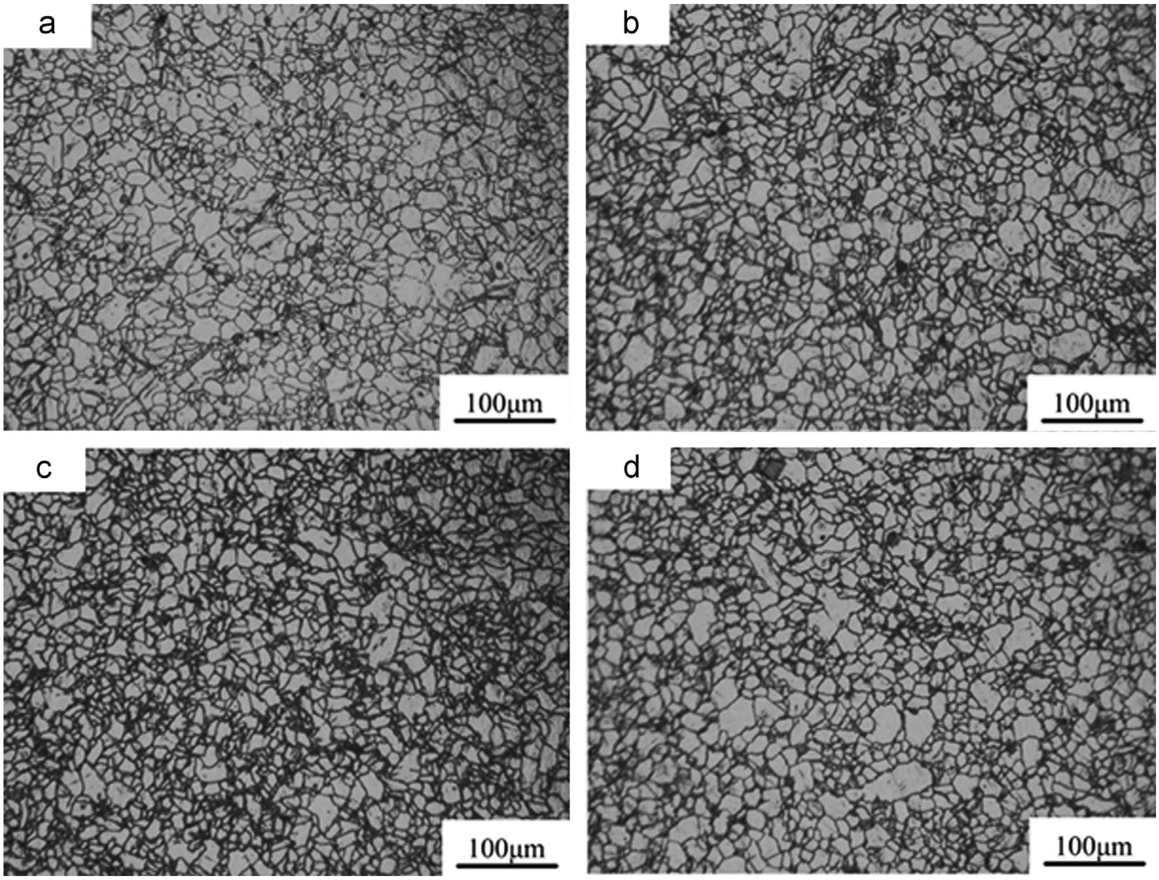

Fig. 5. Optical micrographs of 3% strain PRC AZ31 magnesium alloy samples after inverse tension at different strain rates at 423 K: (a) $10^{-1}\,s^{-1}$, (b) $10^{-2}\,s^{-1}$, (c) $10^{-3}\,s^{-1}$, (d) $10^{-4}\,s^{-1}$.

However, it was very interesting to find that the fracture elongation improved more in PRC samples than in as-received ones despite the reduced ability to activate DXR, except at the strain rates of $10^{-4}\,s^{-1}$ and $10^{-1}\,s^{-1}$. At a strain rate of $10^{-4}\,s^{-1}$, PRC specimens featured equiaxed grains distributed in the microstructure. The grain size was about 14.7 μm, showing very little modification when compared to the original grains (as received, undeformed alloy) of 15.5 μm. The tensile yield strength changed very little between as-received and the PRC sample strained at $10^{-4}\,s^{-1}$. This result might be caused by the long deformation time that made the effects of detwinning insignificant. Besides, at the strain rate of $10^{-4}\,s^{-1}$ there are more fine grains in as-received than in PRC samples, as shown in Fig. 4(d) and Fig. 5(d). Due to finer grain structure, the as-received samples showed a slightly larger fracture elongation than the PRC specimens at strain rate of $10^{-4}\,s^{-1}$. This might be also the reason why the elongation decreased at $10^{-1}\,s^{-1}$ comparing as-received and deformed samples. It can be supposed that DRX was delayed in the pre-deformed samples which led to a reduced softening effect and a smaller fracture elongation. On the contrary, improved elongation ability was measured in the PRC specimens tested at strain rates from $10^{-3}\,s^{-1}$ to $10^{-2}\,s^{-1}$. It might be related to the softening effect caused by grain orientation induced by the twins. In order to confirm the above described trend, further interrupted tests have been performed at different strain rates and the temperature of 423 K, followed by microstructure analyses at an imposed reverse tensile deformation of 5%.

Fig. 6 shows the microstructure and texture of PRC samples after inverse tensile strain of 5% at 423 K with different strain rates of $10^{-1}\,s^{-1}$, $10^{-2}\,s^{-1}$, $10^{-3}\,s^{-1}$, $10^{-4}\,s^{-1}$, respectively. The crystal boundary misorientations of the samples inverse tensile tested with different strain rates at 423 K is shown in Fig. 7. From this collection of micrographs it can be stated that detwinning already took place at 5% strain. At the strain rate of $10^{-1}\,s^{-1}$, detwinning has completed for the faster speed and the larger deformation degree. This is expressed by the typical basal texture observed in Fig. 6(a). As the strain rate decreased from $10^{-2}\,s^{-1}$ down to $10^{-4}\,s^{-1}$, the volume fraction of twins and the texture of formed twins decreased as well. In Fig. 7, it can be seen that the twins are almost tensile twins which are theoretically rotated by ~86°. Fig. 8(a) and (b) shows the enlarged images of 3% PRC and inverse tensile strained 5% samples at $10^{-2}\,s^{-1}$. From the two figures, it can be clearly observed that the thickness of the twinning lamella in the grains became smaller and thinner after inverse tension. In Fig.8(a), the (0002) pole of twinning variants A, B, C, D, E was close to ED which corresponds to {10–12} tensile twins. In Fig. 8(b), the (0002) pole of lamella A, B, C was also close to the ED, thus indicating that during the detwinning behavior, the type of twins was kept same.

Jiang et al. [22] reported the influence of the deformation paths of Mg in two different ways, describing softening and hardening effects. One is that the twin boundaries that have formed acted as barriers to dislocation motion as do grain boundaries, thus leading to an increased work hardening. On the other hand, twin boundaries accommodate strain along the *c*-axis, which gives rise to a decrease in the work hardening rate. The lattice rotation introduced by twinning can also enhance or reduce work hardening depending on the type of twins formed. During the tensile tests along the extrusion direction on AM30 tubes at different temperatures, {10-11}–{10–12} twinning and {10-11} twinning are the dominant deformation modes at moderate temperatures. They reorient the basal planes by 38°and 56°, respectively.

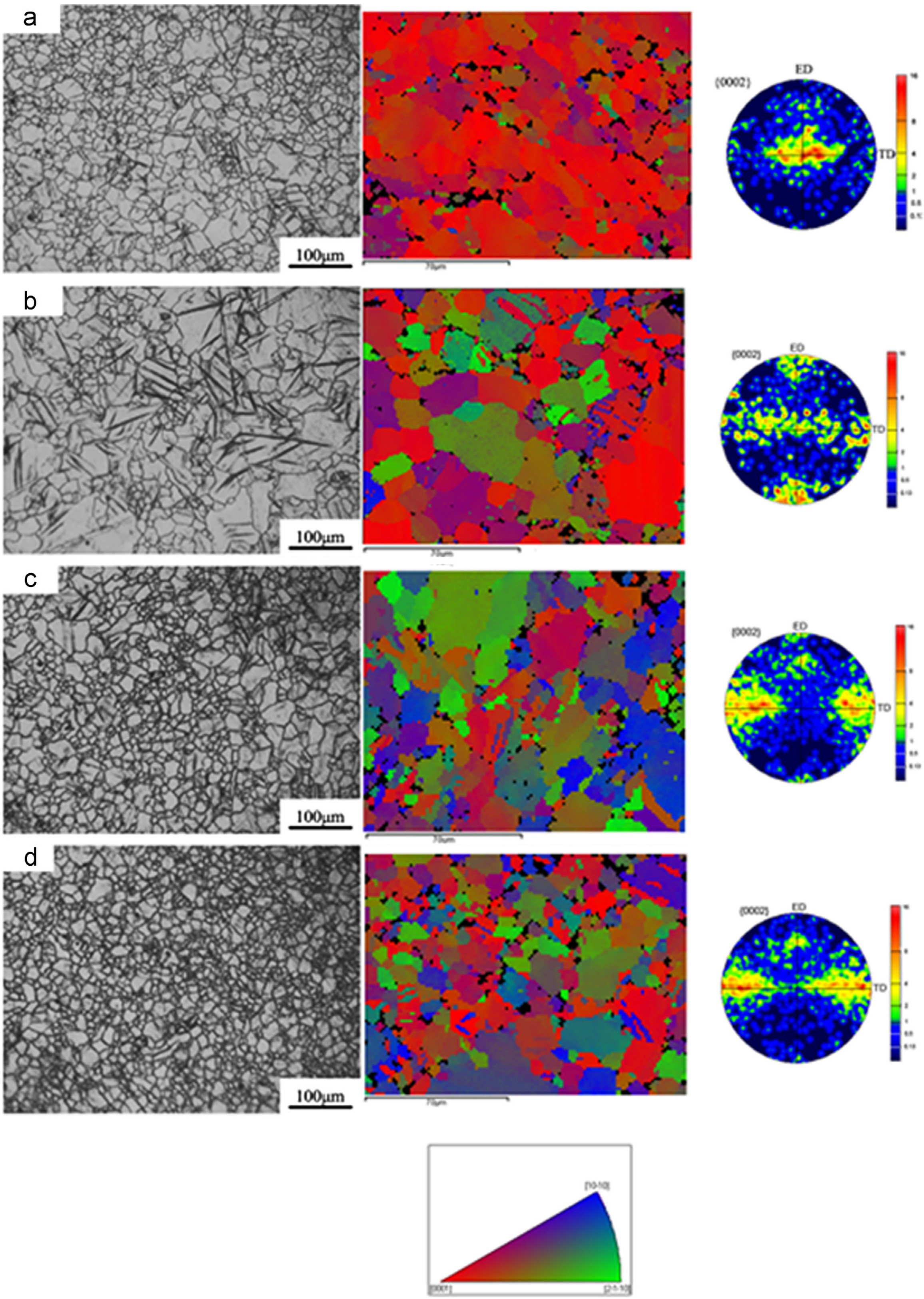

Fig. 6. Optical micrographs and {0002} pole figures of 3% PRC samples subjected to inverse tension to 5% strain at 423 K: (a) $10^{-1}\ s^{-1}$, (b) $10^{-2}\ s^{-1}$, (c) $10^{-3}\ s^{-1}$, (d) $10^{-4}\ s^{-1}$.

The basal planes originally unfavorably oriented for slip can be reoriented to more favorable orientations, which in turn leads to softening. In this case, the twinning-induced softening is more significant than twinning-induced hardening. Barnett et al. [23] indicated that the ductility of magnesium alloys would be improved by extensive {10–12} twinning during the tensile tests owing to the orientation softening effects. It is known that the extension twins re-orient the crystal lattice by ~86° about ⟨11–20⟩

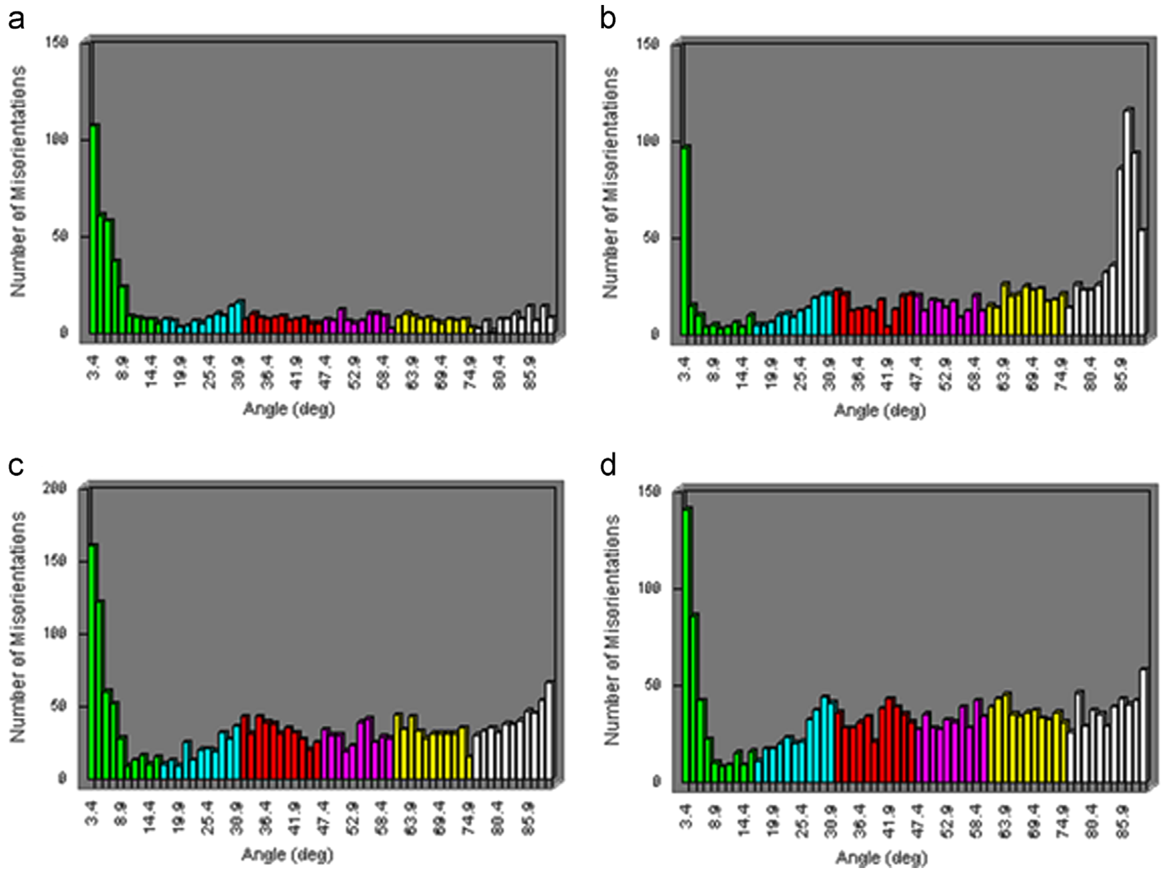

Fig. 7. Misorientation angles at crystal boundaries of the PRC samples subjected to inverse tension at 5% deformation with different strain rates: (a) $10^{-1}\,s^{-1}$, (b) $10^{-2}\,s^{-1}$, (c) $10^{-3}\,s^{-1}$, (d) $10^{-4}\,s^{-1}$.

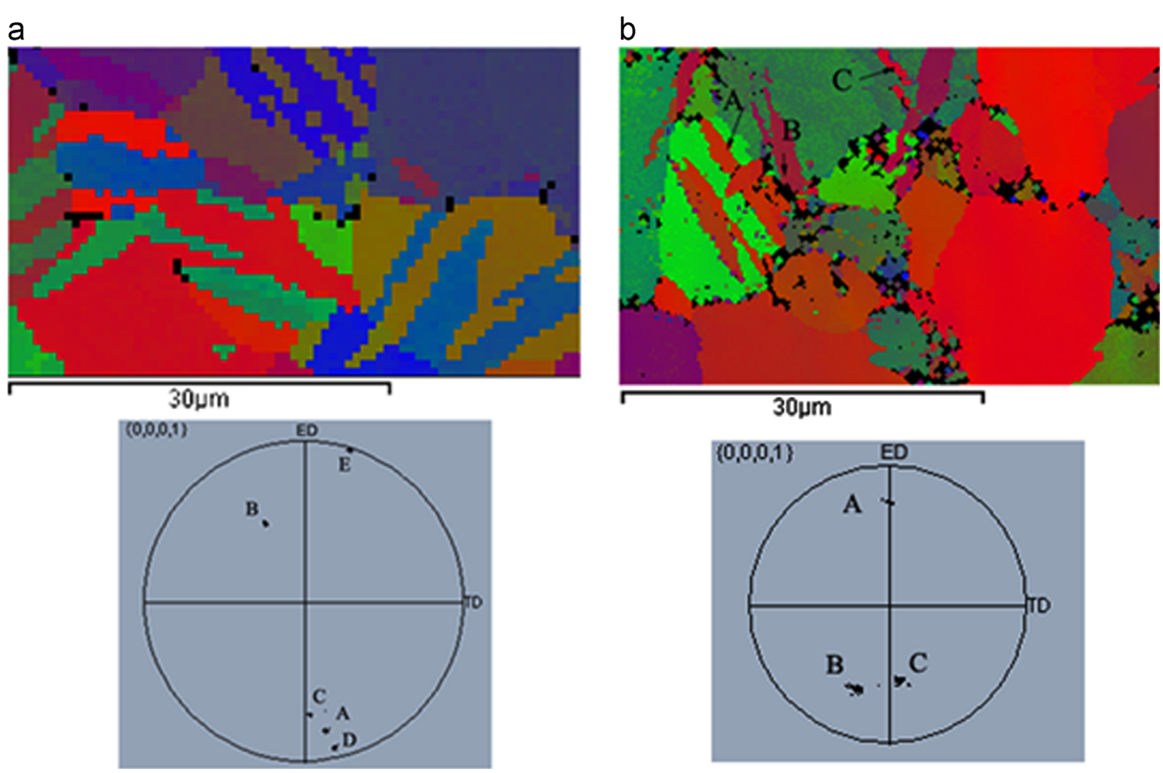

Fig. 8. High magnification EBSD views of (a) 3% PRC, (b) inverse tension at strain rate of $10^{-2}\,s^{-1}$.

direction, as shown in Fig. 7, and it is accepted that after pre-compression, the *c*-axis of grains preferably orients nearly parallel to the extrusion axis [9]. The schematic evolution about the changes of orientation of the grains is depicted in Fig. 9. It is recalled that the preferred orientation achieved by the grains makes the alloy softer by activating the slip systems more easily,

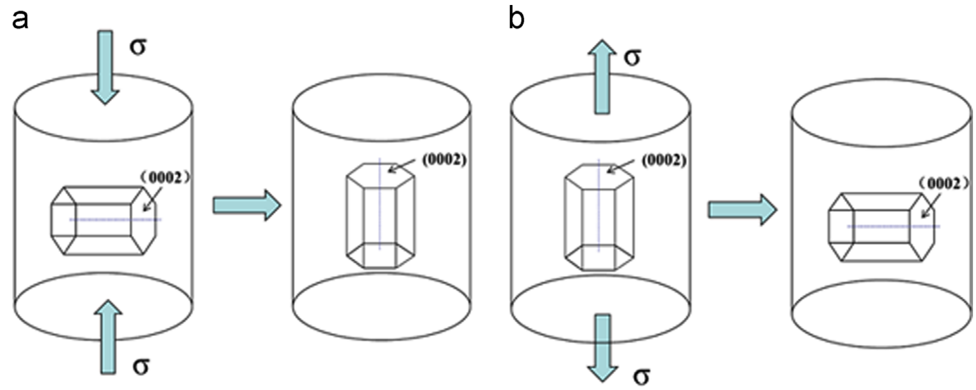

Fig. 9. Schematic picture about the change of the orientation of grains by twinning and detwinning on pre-compression and inverse tensile straining: (a) pre-compression, (b) inverse tension.

thus promoting the observed softening effect during inverse tensile deformation. However, after the twins consumed (i.e. detwinning is completed) it becomes more difficult to further accumulate strain since the orientation would tend to rotate perpendicular to the extrusion axis, as shown in Fig. 9(b). In Fig. 6(a), due to the higher strain rate, the higher stored energy would induce higher detwinning rate which was completed even just at a strain of 5%. As the strain rate decreased from $10^{-2}\,s^{-1}$ to $10^{-4}\,s^{-1}$, more time was available for stress relaxation, so that softening orientation of twins played an important effect on the deformation. In Fig. 6(b), it is confirmed that a large amount of twins is distributed in the microstructure which would contribute to improved plasticity of the alloy. However, the volume fraction of twins decreased as the strain rate decreased. In Fig. 6(c), only a little amount of twins is retained leading to a weaker softening effect and reduced fracture elongation, accordingly.

4. Conclusion

In this paper, the effects of detwinning on the mechanical property of AZ31 extruded magnesium alloy were investigated with different strain rates ranging from $10^{-1}\,s^{-1}$ to $10^{-4}\,s^{-1}$ at 423 K. It has been shown that during inverse tensile tests on the pre-compressed specimens, the detwinning behavior clearly occurred. At 423 K, DRX was delayed by the strain recovery induced by the detwinning process. At the strain rate of $10^{-1}\,s^{-1}$, the detwinning rate was very fast owing to larger stress contraction. As the strain rate decreased from 10^{-2} to $10^{-4}\,s^{-1}$, the detwinning processed was more sluggish and it had little effects at a lower strain rate. The fracture elongation increased as well, except at the strain rates of $10^{-1}\,s^{-1}$ and $10^{-4}\,s^{-1}$. This behavior was accounted for by preferential rotation of the grains that promoted softening in the direction parallel to ED and improvement of fracture elongation after pre-deformation. Furthermore, the highest elongation on pre-deformed samples was obtained at the strain rate of $10^{-2}\,s^{-1}$ owing to the highest amount of residual {10–12} twins which enhanced softening orientation effects.

Acknowledgments

This work was supported by Fundamental Research Funds for the Central Universities (No. CDJZR11130008). Lifei Wang is grateful for financial support of the China Scholarship Council (CSC).

References

[1] M. Knezevic, A. Levinson, R. Harris, R.K. Mishra, R.D. Doherty, S.R. Kalidindi, Acta Mater. 58 (2010) 6230–6242.
[2] Y. Chino, K. Kimura, M. Mabuchi, Mater. Sci. Eng. A 486 (2008) 481–488.
[3] J.C. Baird, B. Li, S.Y. Parast, S.J. Horstemeyer Jr., L.G. Hector, P.T. Wang, M.F. Horstemeyer, Scr. Mater. 67 (2012) 471–474.
[4] J.A. Yasi Jr., L.G. Hector, D.R. Trinkle, Acta Mater. 58 (2010) 5704–5713.
[5] T. Al-Sammana, X. Li, S.G. Chowdhury, Mater. Sci. Eng. A 527 (2010) 3450–3463.
[6] D.L. Yin, J.T. Wang, J.Q. Liu, X. Zhao, J. Alloys Compd. 478 (2009) 789–795.
[7] B. Song, R.L. Xin, G. Chen, X.Y. Zhang, Q. Liu, Scr. Mater. 66 (2012) 1061–1064.
[8] Y.J. Wu, R. Zhu, J.T. Wang, W.Q. Jia, Scr. Mater. 63 (2010) 1077–1080.
[9] Y.N. Wang, J.C. Huang, Acta Mater. 55 (2007) 897–905.
[10] R.L. Xin, B.S. Wang, Z. Zhou, G.J. Huang, Q. Liu, Trans. Nonferrous Met. Soc. China 20 (2010) s594–s598.
[11] H. Zhang, G.S. Huang, J.H. Li, L.F. Wang, Mater. Sci. Forum 747–748 (2013) 352–358.
[12] J.J. He, T.M. Liu, S. Xu, Y. Zhang, Mater. Sci. Eng. A 579 (2013) 1–8.
[13] C. Bruni, A. Forcellese, F. Gabrielli, M. Simoncini, J. Mater. Process. Technol. 210 (2010) 1354–1363.
[14] I.A. Maksoud, H. Ahmed, J. Rödel, Mater. Sci. Eng. A 504 (2009) 40–48.
[15] Y.C. Xin, M.Y. Wang, Z. Zeng, M.G. Nie, Q. Liu, Scr. Mater. 66 (2012) 25–28.
[16] J.A. Valle, O.A. Ruano, Mater. Sci. Eng. A 487 (2008) 473–480.
[17] S.M. Fatemi-Varzaneh, A. Zarei-Hanzaki, H. Beladi, Mater. Sci. Eng. A 456 (2007) 52–57.
[18] S.B. Yi, S. Zaefferer, H.G. Brokmeier, Mater. Sci. Eng. A 424 (2006) 275–281.
[19] G. Proust, C.N. Tomé, A. Jain, S.R. Agnew, Int. J. Plast. 25 (2009) 861–880.
[20] N.L. Li, G.J. Huang, R.L. Xin, Q. Liu, Mater. Sci. Eng. A 569 (2013) 18–26.
[21] W. Wu, S.Y. Lee, A.M. Paradowska, Y.F. Gao, P.K. Liaw, Mater. Sci. Eng. A 556 (2012) 278–286.
[22] L. Jiang, J.J. Jonas, A.A. Luo, A.K. Sachdev, S.P. Godet, Scr. Mater. 54 (2006) 771–775.
[23] M.R. Barnett, Mater. Sci. Eng. A 464 (2007) 1–7.